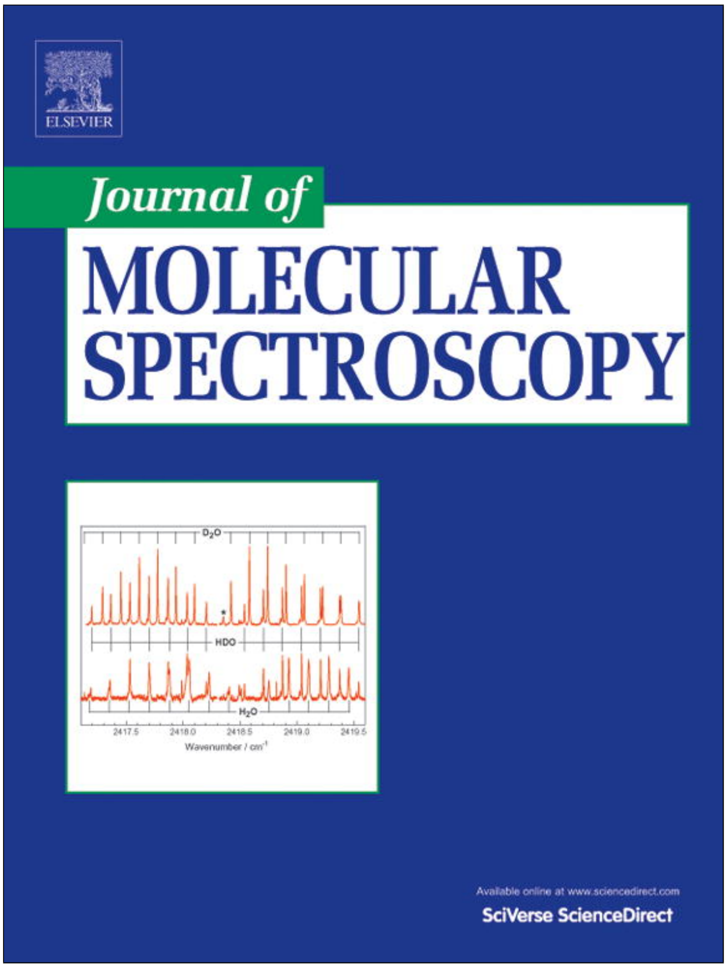

Journal of Molecular Spectroscopy 282 (2012) 1–8

Contents lists available at SciVerse ScienceDirect

Journal of Molecular Spectroscopy

journal homepage: www.elsevier.com/locate/jms

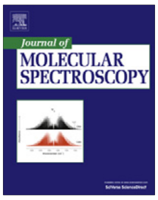

Analysis of an ^{18}O and D enhanced water spectrum and new assignments for $HD^{18}O$ and $D_2{}^{18}O$ in the near-infrared region (6000–7000 cm^{-1}) using newly calculated variational line lists

Michael J. Down [a], Jonathan Tennyson [a,*], Johannes Orphal [b], Pascale Chelin [c], Albert A. Ruth [d]

[a] Department of Physics and Astronomy, University College London, London WC1E 6BT, UK
[b] Karlsruher Institut für Technologie, IMK-ASF, Postfach 36 40, 76021 Karlsruhe, Germany
[c] Laboratoire Interuniversitaire des Systèmes Atmosphériques (LISA), Université de Paris-Est Créteil et Université de Paris-Diderot, CNRS UMR 7583, Créteil, France
[d] Physics Department and Environmental Research Institute, University College Cork, Cork, Ireland

ARTICLE INFO

Article history:
Received 14 February 2012
In revised form 12 September 2012
Available online 10 November 2012

Keywords:
Vibration–rotation spectroscopy
Water
Infrared

ABSTRACT

An experimental infrared spectrum due to Orphal and Ruth (2008) [10] recorded using isotopically enriched water in the 6000–7000 cm^{-1} region is analysed and assigned. The assignment procedure is based on the use of known transition frequencies for $H_2{}^{16}O$ and $H_2{}^{18}O$, existing variational line lists for $HD^{16}O$ and $D_2{}^{16}O$, and newly calculated variational line lists for $HD^{18}O$ and $D_2{}^{18}O$. These new variational line lists are presented herein. The main absorption comes from $HD^{16}O$ and $HD^{18}O$, for which there are few previous assignments in the region. Assignments to 426 new $HD^{18}O$ lines are presented. In all 3254 of the 4768 lines observed in the spectrum are assigned, resulting in a number of newly determined energy levels. These assignments are in agreement with the recent work of Mikhailenko et al. (2012) [41].

1. Introduction

Whilst the spectra of the primary isotopologue of water is well documented [1] there remain gaps in the knowledge of the less abundant water species [2,3]. Although less significant than $H_2{}^{16}O$, the understanding of these rare isotopologues remains important for both terrestrial and stellar atmospheric modelling as well as the completeness of spectroscopic databases. For example isotopologue abundances are often used to trace atmospheric processes since isotopic variations can be caused by specific atmospheric drivers such as cometary and meteorite deposits at the top of the atmosphere. Thus, for example, the trace water isotopologue $HD^{18}O$ has been observed both in the Earth's atmosphere [4] and in the interstellar medium [5], where isotopic abundances vary significantly. In addition, data on isotopically substituted water is essential for the development of theoretical models and in particular helps to characterise effects due to the failure of the Born–Oppenheimer approximation which remains one of the major sources of uncertainty in spectroscopic calculations on water [6,7]. Water isopologue abundances also provide unique information on the atmospheric water cycle [8,9].

Recently Orphal and Ruth [10] obtained a high resolution absorption spectrum of a mixture of $D_2{}^{16}O$ and $H_2{}^{18}O$ gases. While this mixture was designed to maximise the presence of $HD^{18}O$, it actually contains significant quantities of five other isotopologues of water, namely $H_2{}^{18}O$, $HD^{16}O$, $H_2{}^{16}O$, $D_2{}^{18}O$ and $D_2{}^{16}O$ in decreasing order of estimated abundance. The spectrum of $H_2{}^{16}O$ is well characterised in the 6000–7000 cm^{-1} range [11–14]. $H_2{}^{18}O$, the second most abundant naturally occurring isotopologue of water is also well studied in this region [12,14–16]. Conversely the $HD^{18}O$, $D_2{}^{18}O$ and $HD^{16}O$ show yet to be assigned transitions in this spectral region.

For $H_2{}^{18}O$ [2], $HD^{16}O$ and $HD^{18}O$ [3] an IUPAC task group (TG) has provided a comprehensive evaluation of the state of knowledge of the spectroscopy of these species. These compilations provide precise, experimentally-determined energy levels using the so-called MARVEL procedure [17] for these species where possible. These levels provide an excellent starting point for making spectral assignments. Where the upper state energies are yet to be determined experimentally it is possible to use variational line lists to simulate the spectrum and hence to make spectral assignments. There are reliable line lists available for $HD^{16}O$ [18] and $H_2{}^{18}O$ [19]. For $HD^{18}O$ Tomsk [20] provide a line list avilable online based on work by Partridge and Schwenke [21,22], which has been previously employed in similar analyses of this region [23,24] contained in the IUPAC TG dataset. However this was found to be reliable at only the strongest intensities and our own $HD^{18}O$ line list was subsequently computed as part of this work.

The situation for $D_2{}^{16}O$ and $D_2{}^{18}O$ is less clear cut. The IUPAC TG is yet to report on doubly deuterated water isotopologues but, in any case, these are less well characterised spectroscopically than the

---

* Corresponding author. Fax: +44 20 7679 7145.
E-mail address: j.tennyson@ucl.ac.uk (J. Tennyson).

0022-2852/$ - see front matter © 2012 Elsevier Inc. All rights reserved.
http://dx.doi.org/10.1016/j.jms.2012.09.006

other species considered here. However some as yet unpublished $D_2{}^{16}O$ features and around 300 $D_2{}^{18}O$ lines have been assigned in this region by the work of Mikhailenko et al. [25]. Furthermore Ormsby et al. [26] reported assignments of nearly 1800 transitions for $D_2{}^{16}O$. Accurate experimental lower levels are also available both for $D_2{}^{18}O$ [27,28] and $D_2{}^{16}O$ [29]. For $D_2{}^{16}O$ there is a particularly accurate variational line list available due to Shirin et al. [30]. Although there is an online $D_2{}^{18}O$ line list available from Tomsk [20] a new one was computed as part of this work.

This paper is structured as follows. The experimental data available is outlined in Section 2. Section 3 gives the methodology used for our analysis and presents the variational line lists used for the assignments. The results of the analysis and our new assignments are summarised in Section 4. Extensive data sets arising from this work have been placed in the Supplementary data.

2. The observed spectrum

Orphal and Ruth [10] recorded a spectrum in the 6000–7000 cm^{-1} region with a spectral resolution of 0.02 cm^{-1} using a combination of high resolution Fourier Transform (FT) spectroscopy and incoherent broadband cavity-enhanced absorption spectroscopy (IBBCEAS) [31,32]. It should be noted that this spectral resolution does not limit the precision of line positions except in the case of blended lines.

For the measurement the cavity was filled with a gas mixture of 8.0 mbar $D_2{}^{16}O$ and 12.4 mbar $H_2{}^{18}O$. It was let to react for some time at 296 K. The resulting relative abundances of each water isotopologue (listed in Table 1) can be estimated by employing simple statistical arguments based on the partial pressures. It should be noted that fractionation effects, possible presence of contaminants and differential absorption by the walls have been ignored in making these estimates. Over 4700 spectral peaks were observed in the spectrum to a precision of 0.002–0.004 cm^{-1} (in the case of strong isolated lines, in a region with good signal-to-noise ratio). However the strongest lines are affected by saturation, which causes slight broadenings and distortion. The resolution to which saturated and/or blended line positions can be determined will therefore be lower.

The water isotopologue $HD^{18}O$ has been studied before in this spectral region by different techniques with typical absorption path lengths of up to 100 m [13,16]. The absorption sensitivity of FT-IBBCEAS (1σ noise equivalent absorption coefficient at 6504.35 cm^{-1} equals 2.3×10^{-5} cm^{-1}) in combination with the presence of D_2O in the cavity results in the observation of a large number of new absorption features in the spectrum which are notably due to the water isotopologues listed in Table 1. The spectrum provides an excellent starting point for the assignment of the listed species, in particular for $HD^{18}O$, for which the $\nu_1 + \nu_3$, $2\nu_1 + \nu_2$, $2\nu_2 + \nu_3$ triad is centred on this window as can be seen in Fig. 1.

However, the information on line intensities in the spectrum is of rather limited use in the analysis, because absolute intensities are affected by a varying degree of saturation of the strongest lines for the given concentrations of species, especially in the region above 6800 cm^{-1}. It should also be noted that the signal-to-noise ratio is a function of wavenumber in the spectrum, due to the monotonically varying reflectivity of the cavity mirrors across the spectral range [10]. This leads to effective absorption pathlengths of ≈33 m at 6200 cm^{-1}, ≈58 m at 6350 cm^{-1}, ≈180 m at 6500 cm^{-1}, and ≈370 m at 6680 cm^{-1}. Hence, over broad spectral ranges, e.g. many hundreds of wavenumbers, the experimental technique exhibits a gradually varying sensitivity in terms of the maximally achievable signal-to-noise ratio (which moreover also depends on the photon flux from the light source); this fact should however not affect the line intensities per se.

Table 1
Experimental (Expt.) and natural abundances for the six water isotopologues present in the gas mixture of Orphal and Ruth [10]. The experimental abundances are estimated statistically.

Isotopologue	Expt.	Natural
$HD^{18}O$	0.290	6.23×10^{-7}
$H_2{}^{18}O$	0.225	1.99×10^{-3}
$HD^{16}O$	0.186	3.11×10^{-4}
$H_2{}^{16}O$	0.145	0.977
$D_2{}^{18}O$	0.093	4.90×10^{-11}
$D_2{}^{16}O$	0.060	2.42×10^{-8}

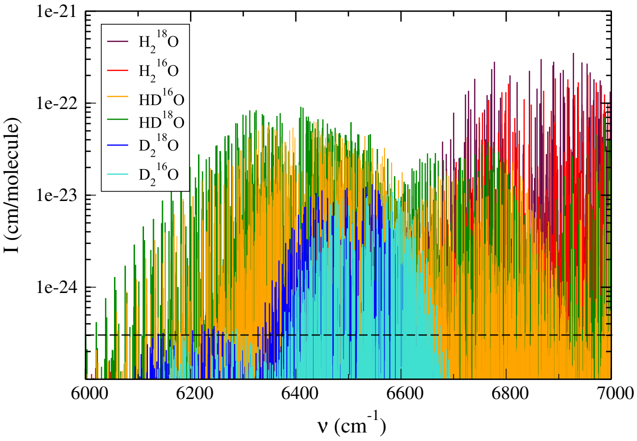

Fig. 1. The combination of selected data sources for the six isotopologues of water in the 6000–7000 cm^{-1} region. Intensities are scaled by the estimated experimental abundances given in Table 1 and the dashed line indicates the intensity cut off.

3. Analysis

Our approach for assigning the previously unobserved lines in the spectrum is to first identify and remove previously observed lines from the experimental line list. This was done by comparison with spectroscopic databases [3,33]. As shown below, this step also allowed us to calibrate the observed spectrum.

While traditional methods of spectral analysis employ combination differences (CDs) as the major method for assigning spectra, the large number of lines, presence of six different species and the fact that line positions could only be determined to 0.002 cm^{-1} meant that the danger of false positive CD's is high. Lack of resolution in general exacerbates this problem, since estimated precisions are lower for blended lines. Conversely, the accuracy of computed line lists allows assignments to be made confidently by comparison with calculations. New assignments were therefore made by comparison with variational line lists for which a combination of published [18,30] and newly computed lists were used. Checks and further assignments were then made using CD's.

These procedures are detailed in the following subsections.

3.1. Data sources

Since the spectra of $H_2{}^{16}O$ and $H_2{}^{18}O$ are well documented at the wavelengths and intensities required spectroscopic data taken from HITRAN [33] was initially used for these species. This proved insufficient to identify all the $H_2{}^{18}O$ lines and the analysis for this species was repeated using a new $H_2{}^{18}O$ line list due to Lodi and Tennyson [19]. This line list was calculated using DVR3D [34], the very recent spectroscopically-determined potential energy surface (PES) of

Bubakina et al. [35], and the high accuracy LTP2011 dipole moment surface (DMS) of Lodi et al. [36]. This line list has the unusual feature that the computed energy levels are replaced by empirically-determined ones from the IUPAC TG [3] where possible.

Partition functions for $H_2{}^{16}O$, $H_2{}^{18}O$, $HD^{16}O$ and $HD^{18}O$ were taken from HITRAN, but otherwise there is no HITRAN data to aid the line assignments of the rarer isotopologues and thus other line lists had to be found. The partition function for $D_2{}^{16}O$ was taken from Shirin et al. [30] whilst a value for $D_2{}^{18}O$ was taken from Tomsk data on line.

For $D_2{}^{16}O$ the line list of Shirin et al. [30] was used. This is also based on DVR3D calculations and an empirical PES. This line list claims an accuracy of 0.023 cm^{-1} and our assigned line positions agreed with the observations within a 0.04 cm^{-1} error. There is also a $D_2{}^{16}O$ line list available from Tomsk [20] which is based on the PES and DMS of Partridge and Schwenke [21,22]. Comparison showed that this line list was much less reliable for all but the strongest lines. Use of Tomsk line lists was therefore not pursued.

For $HD^{16}O$ the VTT line list of Voronin et al. [18] was used to make assignments. This line list was calculated using DVR3D, a semi-empirical PES [37] and the CVR DMS [38]. In each case a small constant frequency shift was necessary in order to bring each line list into agreement with observation. These shifts resulting from a combination of a small systematic experimental error and, for the theoretical line lists, any systematic error associated with the calculations will be examined further below.

3.2. Variational calculations

Line lists for $HD^{18}O$ and $D_2{}^{18}O$, were computed as part of this work using DVR3D [34].

Calculations for $HD^{18}O$ were based on the previous work of Voronin et al. [18,37] on $HD^{16}O$. Our calculations were performed up to $J = 14$ in Radau coordinates with input parameters derived from the tested values of Voronin et al. [18]; this ensured convergence of results well above the energies considered here. Their empirically tuned $HD^{16}O$ PES [37] was also used and intensities were calculated using the LTP2011 DMS [39]. The computed line list compared well with the available HITRAN data and to our knowledge is the best currently available for this isotopologue. The entire 296 K $HD^{18}O$ line list between 0 and10 000 cm^{-1} has been placed in the Supplementary material.

Calculations for $D_2{}^{18}O$ were carried out using the PES of Shirin et al. [30] in their variational calculations for $D_2{}^{16}O$, with masses appropriate for $D_2{}^{18}O$. Again the LTP2011 DMS was used [39]. Calculations were performed up to $J = 15$ in symmetrised Radau coordinates with DVR3D input parameters based on the $D_2{}^{16}O$ calculations of Shirin et al. The computed line list proved useful in assigning the spectrum and we believe it to be more accurate than the line list of Tomsk on line. We therefore include the entire 296 K $D_2{}^{18}O$ line list between 0 and 10 000 cm^{-1} in the Supplementary material.

A spectrum in the 6000–7000 cm^{-1} region for all the selected line lists appear in Fig. 1 where all intensities are scaled by the experimental abundances. It is clear from this figure that $D_2{}^{16}O$ and $D_2{}^{18}O$ provide very little of the absorbed intensity in this spectral region. Furthermore the peak of $H_2{}^{16}O$ and $H_2{}^{18}O$ intensities are found towards the high wave number end of the region and as a result the main absorption comes from the $HD^{16}O$ and $HD^{18}O$ isotopologues.

3.3. Method

Statistical arguments suggest the experiment involves six possible isotopologues in the approximate abundances shown in Table 1. To account for these relative abundances the intensities of all lines used in the analysis were scaled by these factors and a uniform intensity cut off applied at 3×10^{-25} cm/molecule. This left 5472 lines in total from all sources to be included in the analysis. This cut off was chosen to provide enough lines to account for all observed features whilst minimising the line density of the spectrum.

As a starting point a line list was constructed which simulated the experimental observations. This used data from HITRAN 2008 and the chosen variational calculations. The process of removing known lines was based on a direct matching routine which compares positions of observed peaks and known lines within a frequency interval, with the possibility of a constant frequency shift being applied. The chance that lines match coincidentally is deemed to be small for the line density of this spectrum and the small frequency intervals employed. The presence of a large number of matches found within a small frequency interval was used to determine an appropriate shift for each line list and the matching frequency range was then trimmed correspondingly to minimise the chance of coincidental matches. The presence of structure in the residuals, see Figs. 3 and 5, supports the validity of matches as the visible rotational structure of the assigned lines correlates to rotational structure in the residual plots. This is to be expected as with these types of variational calculations $\nu_{obs} - \nu_{calc}$ errors vary smoothly with J, K_a and K_c [40]. In some cases vibrational structure is also visible.

At this point several considerations should be noted. Firstly there is potential for blended lines and many blended pairs are noted below. However weak lines contributing less than 9% of the intensity of a pair have been ignored and are not assigned here. Secondly, while weaker lines may be hidden by a blend, or indeed if very weak, by noise, it should be possible to account for all of the strong observed peaks with the compiled data set. These considerations in part explain the excess of unassigned weak observed peaks at the end of the analysis whilst the vast majority of strong lines are accounted for. Finally, it is possible when employing this strategy that previously unobserved features can be missed when they coincide with known lines and are blended. In this scenario the known line is matched to the observed peak which is removed from the observed data before new features are looked for. In some cases the known line may actually be the part of a pair of blended lines and leave us with a strong predicted feature which is not assigned to an observation.

As a final verification of our assignments all new upper energies were checked via CD relations.

4. Results and discussion

4.1. Initial analysis

Lines belonging to the well documented $H_2{}^{16}O$ isotopologue were the first to be analysed using the 566 lines with intensities greater than the threshold taken from HITRAN [33]. The plot of the residuals given in Fig. 2 clearly shows a shift of $\nu_{obs} - \nu_{HITRAN} = -0.019$ cm^{-1} between the observed and HITRAN positions for the vast majority of assigned lines. Correcting this shift and using a matching interval of 0.015 cm^{-1} assigned 304 $H_2{}^{16}O$ lines including 10 blended lines.

The remaining observed lines were then compared with the $H_2{}^{18}O$ line list [36]. Again the vast majority of assigned lines showed residuals of around $\nu_{obs} - \nu_{Lodi} = -0.019$ cm^{-1} as shown in Fig. 2 and it was necessary to correct this shift. A matching frequency interval of 0.015 cm^{-1} was again used for the assignment. From the initial set of 704 $H_2{}^{18}O$ lines predicted above the intensity cut off, 346 lines including 31 blends were assigned to $H_2{}^{18}O$. It should be noted that since we made no new assignments to $H_2{}^{18}O$ all line positions in the line list for this species are effectively experimental ones [19].

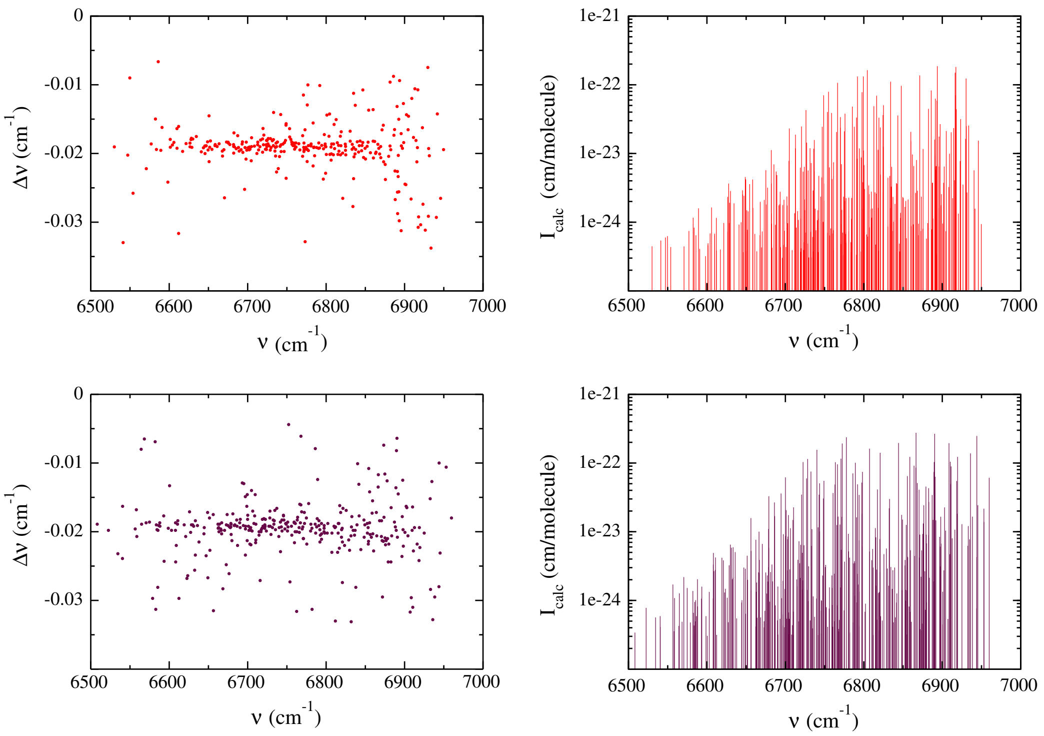

Fig. 2. Upper: Residuals of observed – HITRAN line positions for $H_2{}^{16}O$ (left) and the assigned $H_2{}^{16}O$ features which were removed from the analysis (right). Lower: Residuals of observed –MARVEL line positions for $H_2{}^{18}O$ (left) and the assigned $H_2{}^{18}O$ features removed from the analysis (right).

The presence of the same small shift in both these cases indicates a small systematic experimental error of $-0.019\ \text{cm}^{-1}$ which is within the experimental resolution of $0.02\ \text{cm}^{-1}$. This was considered in all subsequent assignments and all our results were re-calibrated by this value.

Next features belonging to the doubly deuterated isotopologues were removed from the spectrum. First the strongest 295 lines from the $D_2{}^{16}O$ line list and a matching frequency interval of $0.04\ \text{cm}^{-1}$ were used. The 265 line assignments of which 40 are blended were dominated by the $\upsilon_1 + \upsilon_2 + \upsilon_3$ band. These calculations required a further constant shift of $-0.045\ \text{cm}^{-1}$ as well as the systematic experimental error correction. The extra shift is roughly comparable to the quoted band error for $\upsilon_1 + \upsilon_2 + \upsilon_3$ at $\nu_{obs} - \nu_{calc} = 0.02\ \text{cm}^{-1}$ [30]. The residuals for these assignments show rotational structure, see Fig. 3. In particular, these features clearly correlate with the P, Q and R branch structure of the assigned lines.

Our variational calculations for $D_2{}^{18}O$ predicted 337 lines above the intensity cut off in this region. The assignment was carried out within a $0.03\ \text{cm}^{-1}$ interval, no shift being necessary following the usual recalibration. Of these calculated lines 233 could be assigned directly to observations including 38 blended lines. Again the residuals show the expected rotational structure as seen in Fig. 3.

The VTT line list, used to assign the observed $HD^{16}O$ features, predicts 1692 lines above the intensity cut off in the region. Assignment was carried out with a $-0.035\ \text{cm}^{-1}$ shift applied to the calculations. Again the shift was comparable to the quoted band errors in the calculations [37] (typically $0.018\ \text{cm}^{-1}$). A 1284 lines were matched including a number of new assignments, and 305 blended lines. Again the residuals show rotational structure as shown in Fig. 5 and several vibrational bands can be seen.

Finally our $HD^{18}O$ line list predicts 1952 lines stronger than the intensity cut off in the 6000–7000 cm^{-1} region. This resulted in 1224 assignments including 406 blended lines. The calculations required a shift of $-0.04\ \text{cm}^{-1}$ after recalibration and a frequency interval of $0.06\ \text{cm}^{-1}$ was used in making assignments. Again the rotational structure of the residuals can clearly be seen in Fig. 5 where structure due to several vibrational bands can also be identified.

An assigned and labelled sample of the spectrum is shown in Fig. 4 with arbitrary intensity units for the continuous experimental spectrum. In this region all of the main features are assigned. Here the assignment process is obvious. For the sake of clarity assignments are plotted with the observed position rather than that calculated. The analysis left 1514 unassigned lines shown in Fig. 6 against the original 4738 observed lines. It is clear that the majority of strong lines are either already assigned or are assigned for the first time in this work.

The results are summarised in Table 2. The number of lines assigned to each isotopologue reflect their respective abundances in the experiment and the general features of Fig. 1. It should also be noted that the blended pairs quoted only refer to blends within a single isotopologue. Blends between isotopologues have not been explicitly treated here and so it is possible that $HD^{18}O$ features have been missed in favour of the other isotopologues (predominantly $HD^{16}O$). As an example switching the order of the final assignment of $HD^{16}O$ and $HD^{18}O$ species suggests as many as 200 lines are blended between these two species.

4.2. New assignments

An observed line list, both original and recalibrated, with assignments is given in the Supplementary material; these results are summarised in Table 3. No new assignments were made for $H_2{}^{16}O$. This is unsurprising as the spectrum of this species is already well documented. For $H_2{}^{18}O$ no new lines were observed and indeed the energy levels involved are well documented by the IUPAC TG [2,3]. Assignments for $HD^{16}O$ and $HD^{18}O$ were compared against the existing IUPAC TG data, taken as the latest compilation of reliable assignments, to remove known assignments. It should be noted at this point that for $HD^{16}O$ the vibrational labellings provided for the upper levels by Voronin et al. [18] were not in agreement with those of the IUPAC TG data for 30 transitions.

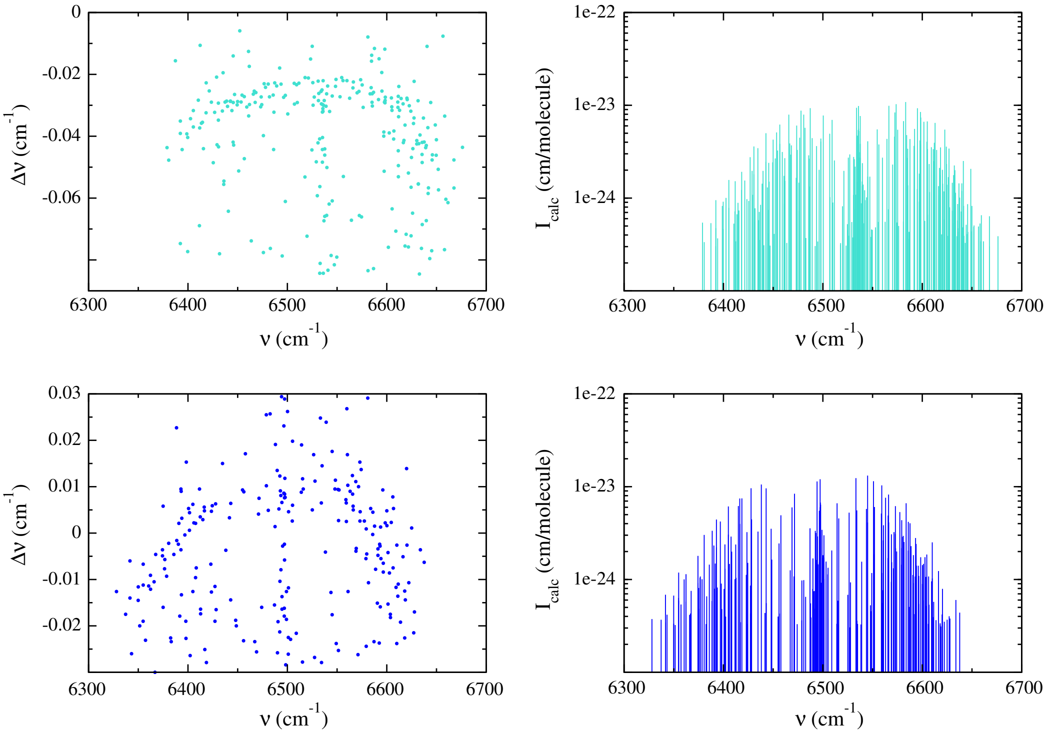

Fig. 3. Upper: Residuals of obs − calc line positions for $D_2{}^{16}O$ assignments (left) and the assigned features of $D_2{}^{16}O$ removed from the analysis (right). Lower: Residuals of obs − calc line positions for $D_2{}^{18}O$ assignments (left) and the $D_2{}^{18}O$ assignments removed from the analysis (right).

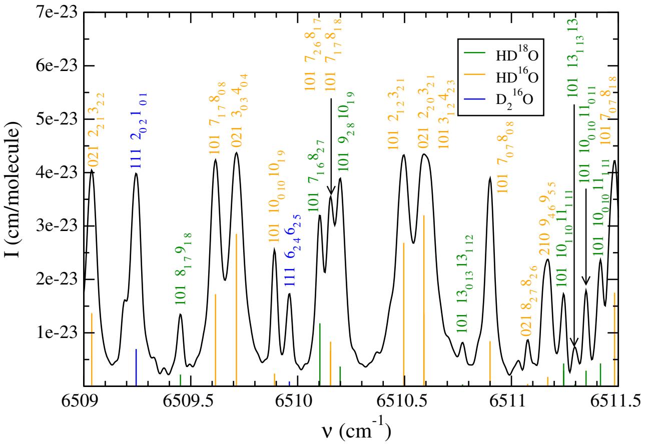

Fig. 4. An assigned and labelled sample of the spectrum between 6509 and 6511.5 cm^{-1}. The continuous line represents the observed spectrum whilst sticks of different colour represent each isotopologue. The intensity scale refers to the calculated lines given as the height of the sticks. Labels are given in the format $\upsilon_1''\upsilon_2''\upsilon_3''\ J'_{K'_aK'_c}\ J''_{K''_aK''_c}$ where $'$ and $''$ represent lower and upper states respectively. Note the blended pairs of assignments arising from doublets.

As expected there were many (426) new assignments for $HD^{18}O$ not present in IUPAC TG dataset although all but 29 $HD^{16}O$ assignments were already present. The previous work of Ormsby et al. [26] in this region assigns all the $D_2{}^{16}O$ transitions observed here, however for $D_2{}^{18}O$ 174 new assignments were made to complement the work of Mikhailenko et al. [25].

4.3. Labelling

An effort has been made to fully label the previously unobserved transitions which predominantly belong to $HD^{18}O$, with standard but approximate normal mode, rigid rotor labels. The variational calculations used only employ rigorous quantum numbers for the energy levels, namely J and p for HDO, as well as ortho/para for H_2O and D_2O. This is sufficient to assign new spectral features. However in order to fully label newly observed energy levels, augmenting the calculated rigorous quantum numbers with normal vibrational modes and K_a and K_c quantum numbers is necessary.

For both $HD^{16}O$ and $D_2{}^{16}O$ the line lists [18,30] already have approximate labels which for $D_2{}^{16}O$ are adopted here. However in the case of $HD^{16}O$, labels from the VTT line list were found to be inconsistent with the IUPAC TG data for 30 transitions and for these we adopt the IUPAC TG labellings.

Labels for $HD^{18}O$ assignments came from the necessarily labelled energy levels of the IUPAC TG [2,3]. These were matched with the DVR3D calculated energy levels based on rigorous quantum numbers and energies as Fig. 7 shows. Levels were matched within +0.1 and −0.04 cm^{-1} of a curve fitted quadratically to the error trend as a function of frequency. The only consideration here was that of degenerate $K_a = 0$, 1 and $K_c = J$ energy level pairs which could not be matched uniquely automatically. The figure shows well-defined vibrational and rotational structure which should be expected with calculations of this type and therefore supports the labellings. This process labelled all observed energy levels except a handful of upper energies which are therefore observed for the first time. These unlabelled levels could therefore potentially give rise to further line assignments via CD's.

For the $D_2{}^{18}O$ assignments lower labels were provided by comparison with an established set of lower energy levels from Ref. [27]. Upper labels could then be found by comparison with the published levels of Mikhailenko et al. [25] in many cases.

4.4. Combination differences and energy levels

All new assignments have been checked via combination differences on upper energy levels and agreement only accepted better than 0.1 cm^{-1}. This involves using a set of reliable experimental lower energy levels and the set of assigned transitions to compute

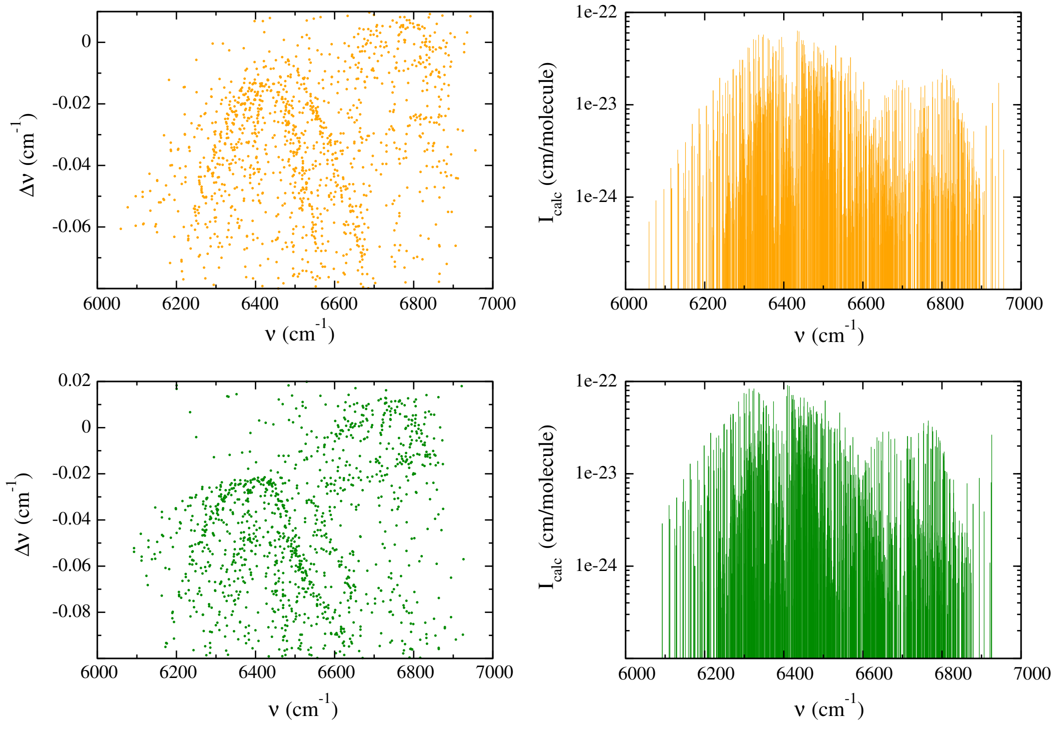

Fig. 5. First Row: Residuals of obs – calc line positions for $HD^{16}O$ assignments (left) and the lines assigned as a result of the analysis (right). Second Row: Residuals of obs – calc line positions for $HD^{18}O$ assignments (left) and the lines assigned as a result of the analysis (right).

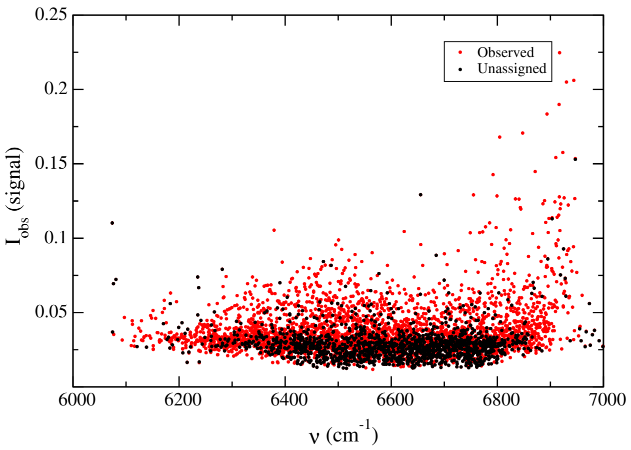

Fig. 6. A comparison of all observed peaks and those 1512 remaining unassigned after the analysis. The majority of strong peaks in this region are now assigned.

Table 2
A summary of the initial analysis indicating for each isotopologue present the number of lines included in the analysis, being above the intensity threshold of 3 × 10^{-25}, the number of lines observed in the spectrum,the number of lines thought to be blended with others from the same species and the reference of the sources used in each case.

Isotopologue	Included	Assigned	Blended lines	Line list reference
$H_2{}^{16}O$	566	304	10	HITRAN [33]
$H_2{}^{18}O$	704	343	28	Lodi et al. [36]
$HD^{18}O$	1952	1224	406	This work
$HD^{16}O$	1692	1284	305	VTT [18]
$D_2{}^{18}O$	337	233	38	This work
$D_2{}^{16}O$	295	265	40	Shirin et al. [30]
Totals	5546	3653	827	

Table 3
A summary of assignments made for each isotopologue. The number of new assignments and labellings are noted.

Isotopologue	Assigned	New	Labelled
$HD^{18}O$	1224	426	1224
$HD^{16}O$	1284	29	1284
$D_2{}^{18}O$	233	174	195
Totals	2741	629	2703

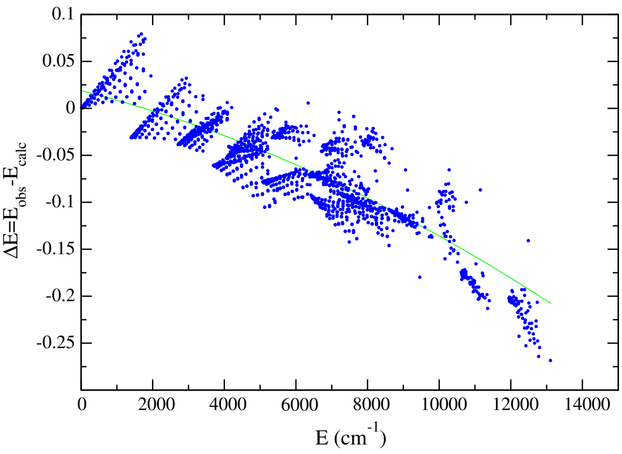

Fig. 7. Residuals of matching between fully labelled MARVEL energy levels and our DVR3D calculations based on rigorous quantum numbers as well as energy. Matches were made within +0.1 cm^{-1} and −0.05 cm^{-1} of a quadratic fit (green). (For interpretation of the references to colour in this figure legend, the reader is referred to the web version of this article.)

all possible upper energies. All occurrences of a labelled upper energy level should then agree to within a certain limit. Bad agreement was initially checked for blends and, especially for weak lines, a number of tentative assignments were removed.

Table 4
A summary of upper energy levels observed for each isotopologue. The number of new levels and the number confirmed by CD's are noted.

Isotopologue	Upper Levels	CD confirmed	New
$HD^{18}O$	412	296	86
$HD^{16}O$	412	299	10
$D_2{}^{18}O$	154	64	102
Totals	978	659	200

For $HD^{16}O$ and $HD^{18}O$ the IUPAC energy levels were used as a basis and CD's required to agree to within 0.1 cm^{-1}, in keeping with the largest experimental errors we expect. For $HD^{18}O$ a total of three assignments with deviations between 0.1 cm^{-1} and 0.12 cm^{-1} were permitted on the basis that weak blended lines have greater experimental uncertainties. For $D_2{}^{18}O$ the lower levels of Liu et al. [27] were employed and all CD's found to agree better than 0.1 cm^{-1}, over 99% having agreement better than 0.05 cm^{-1}. The process of CD checking upper energies provides a list of all upper levels assigned. These levels are available as part of the Supplementary material and are presented alongside the number of transitions to which they belong and the average square CD error of the level. Cases for which an energy level only belongs to one assigned transition are also included but noted as unconfirmed by CD's. These assignments must be regarded as less secure.

The results of the CD's analysis are summarised in Table 4 for each isotopologue. Newly observed energy levels were found for the isotopologues $HD^{18}O$, $HD^{16}O$ and $D_2{}^{18}O$.

5. Conclusions

Our analysis has made a large number of assignments to the six primary water isotopologues. For $HD^{18}O$ and $D_2{}^{18}O$ many of the transitions prove to be previously unobserved. Energy levels are also observed for the first time for these two isotopologues and an effort has been made to provide the standardised labels for the new assignments and energy levels where possible. CD's has also been employed to check our assignments which are predominantly based on line list comparisons.

The assigned spectrum with all assignments (existing and new) and all known labels is provided in the Supplementary material. We hope it to be of use in any future analysis of this spectral region and a valuable part of any spectroscopic database. Additionally we provide the labelled energy levels and their CD statistics for each isotopologue which should also be of use in further spectral analysis of these isotopologues. All transitions frequencies are re-calibrated by the addition of 0.019 cm^{-1} to the observed frequencies. This recalibration therefore also corresponds to corrected upper state energies as a result of CD's.

Over 3200 of the observed peaks have been assigned representing the vast majority of strong features in the spectrum leaving. The remaining 1514 features could be due to trace species such as $H_2{}^{17}O$ or minute quantities of contaminants that may have been present in the water samples. However, following the comparison of the remaining features with the HITRAN data for $H_2{}^{17}O$ yielding assignments to only a handful of weak lines, assignment of this species was not pursued.

After completion of this work Mikhailenko et al. [41] presented an analysis of an isotopically enriched water spectrum in the 6000–9200 cm^{-1} region recorded using a Fourier Transform spectrometer set up as detailed in Refs. [42,43]. Their sample had a higher proportion of deuterium than the one analysed here and gave estimated concentrations of 0.1558 and 0.7368 for $HD^{18}O$ and $D_2{}^{18}O$, for which they found respectively 2596 and 3436 lines in the entire region they studied. Comparison with our results shows very substantial overlap and agreement between the two studies. Indeed the majority of our claimed new transitions were also observed by Mikhailenko et al. Only 26 transitions of $HD^{18}O$ and 38 transitions of $D_2{}^{18}O$ assigned here are not present in their analysis. Furthermore no new upper levels are observed for $HD^{18}O$ and only 36 new upper levels are observed for $D_2{}^{18}O$ relative to the recently published work of Mikhailenko et al. Vibrational labellings for $HD^{16}O$ were also found to differ between Mikhailenko et al. and this work in two cases.

A detailed comparison between the measurements highlights frequency discrepancies between the two spectra which are greater than the claimed accuracy of the Mikhailenko et al.; this is likely to be due to blending and saturation effects in the present experiment. This is realised by a number of upper level inconsistencies up to 0.12 cm^{-1} for $HD^{18}O$ and 0.1 cm^{-1} for $D_2{}^{18}O$. In a small number of cases this gives rise to discrepancies between derived upper levels and those of Mikhailenko et al. larger than the claimed accuracy of 0.015 cm^{-1}.

Acknowledgments

Michael J. Down thanks NERC for a studentship. This work is supported by ERC Advanced Investigator Project 267219. A. Ruth acknowledges support from the Irish EPA (Grant: STRIVE 2008-FS-EH-2-S5). We also acknowledge the help of N.F. Zobov in obtaining the $D_2{}^{18}O$ PES employed here.

Appendix A. Supplementary material

Supplementary data for this article are available on ScienceDirect (www.sciencedirect.com) and as part of the Ohio State University Molecular Spectroscopy Archives (http://library.osu.edu/sites/msa/jmsa_hp.htm). Supplementary data associated with this article can be found, in the online version, at http://dx.doi.org/10.1016/j.jms.2012.09.006.

References

[1] P.F. Bernath, Phys. Chem. Chem. Phys. 4 (2002) 1501–1509.

[2] J. Tennyson, P.F. Bernath, L.R. Brown, A. Campargue, M.R. Carleer, A.G. Császár, R.R. Gamache, J.T. Hodges, A. Jenouvrier, O.V. Naumenko, O.L. Polyansky, L.S. Rothman, R.A. Toth, A.C. Vandaele, N.F. Zobov, L. Daumont, A.Z. Fazliev, T. Furtenbacher, I.E. Gordon, S.N. Mikhailenko, S.V. Shirin, J. Quant. Spectrosc. Radiat. Transf. 110 (2009) 573–596.

[3] J. Tennyson, P.F. Bernath, L.R. Brown, A. Campargue, M.R. Carleer, A.G. Császár, L. Daumont, R.R. Gamache, J.T. Hodges, O.V. Naumenko, O.L. Polyansky, L.S. Rothman, R.A. Toth, A.C. Vandaele, N.F. Zobov, A.Z. Fazliev, T. Furtenbacher, I.E. Gordon, S.N. Mikhailenko, B.A. Voronin, J. Quant. Spectrosc. Radiat. Transf. 111 (2010) 2160–2184.

[4] Z. Zelinger, B. Barret, P. Kubt, P. Ricaud, J.-L. Attie, E. Le Flochmon, J. Urban, D. Murtagh, M. Stik, Mol. Phys. 104 (2006) 2815–2820.

[5] E.A. Bergin, T.G. Phillips, C. Comito, N.R. Crockett, D.C. Lis, P. Schilke, S. Wang, T.A. Bell, G.A. Blake, B. Bumble, E. Caux, S. Cabrit, C. Ceccarelli, J. Cernicharo, F. Daniel, T. de Graauw, M.-L. Dubernet, M. Emprechtinger, P. Encrenaz, E. Falgarone, M. Gerin, T.F. Giesen, J.R. Goicoechea, P.F. Goldsmith, H. Gupta, P. Hartogh, F.P. Helmich, E. Herbst, C. Joblin, D. Johnstone, J.H. Kawamura, W.D. Langer, W.B. Latter, S.D. Lord, S. Maret, P.G. Martin, G.J. Melnick, K.M. Menten, P. Morris, H.S.P. Müller, J.A. Murphy, D.A. Neufeld, V. Ossenkopf, L. Pagani, J.C. Pearson, M. Pérault, R. Plume, P. Roelfsema, S.-L. Qin, M. Salez, S. Schlemmer, J. Stutzki, A.G.G.M. Tielens, N. Trappe, F.F.S. van der Tak, C. Vastel, H.W. Yorke, S. Yu, J. Zmuidzinas, Astr. Astrophys. 521 (2010) L20.

[6] P. Barletta, S.V. Shirin, N.F. Zobov, O.L. Polyansky, J. Tennyson, E.F. Valeev, A.G. Császár, J. Chem. Phys. 125 (2006) 204307.

[7] N.F. Zobov, S.V. Shirin, L. Lodi, B.C. Shirin, J. Tennyson, A.G. Császár, O.L. Polyansky, Chem. Phys. Lett. 507 (2011) 48–51.

[8] J. Steinwagner, S. Fueglistaler, G. Stiller, T. Clarmann, M. Kiefer, P. Borsboom, A. van Delden, T. Röckmann, Nature Geosci. 3 (2010) 262–266.

[9] M. Schneider, K. Yoshimura, F. Hase, T. Blumenstock, Atmos. Chem. Phys. 10 (2010) 3427–3442.

[10] J. Orphal, A.A. Ruth, Opt. Express 16 (2008) 19232–19243.

[11] R.A. Toth, Appl. Opt. 33 (1994) 4852–4867.

[12] P. Macko, D. Romanini, S.N. Mikhailenko, O.V. Naumenko, S. Kassi, A. Jenouvrier, V.G. Tyuterev, A. Campargue, J. Mol. Spectrosc. 227 (2004) 90–108.

[13] A. Jenouvrier, L. Daumont, L. Régalia-Jarlot, V.G. Tyuterev, M. Carleer, A.C. Vandaele, S. Mikhailenko, S. Fally, J. Quant. Spectrosc. Radiat. Trans. 105 (2007) 326–355.
[14] S.N. Mikhailenko, W. Le, S. Kassi, A. Campargue, J. Mol. Spectrosc. 244 (2007) 170–178.
[15] J.-P. Chevillard, J.-Y. Mandin, C. Camy-Peyret, J.-M. Flaud, Can. J. Phys. 64 (1986) 746–761.
[16] A.-W. Liu, J.-H. Du, K.-F. Song, L. Wang, L. Wan, S.-M. Hu, J. Mol. Spectrosc. 237 (2006) 149–162.
[17] T. Furtenbacher, A.G. Császár, J. Tennyson, J. Mol. Spectrosc. 245 (2007) 115–125.
[18] B.A. Voronin, J. Tennyson, R.N. Tolchenov, A.A. Lugovskoy, S. Yurchenko, Mon. Not. R. Astr. Soc. 402 (2010) 492–496.
[19] L. Lodi, J. Tennyson, J. Quant. Spectrosc. Radiat. Trans. 113 (2012) 850–858.
[20] http://spectra.iao.ru, 2012.
[21] H. Partridge, D.W. Schwenke, J. Chem. Phys. 106 (1997) 4618–4639.
[22] D.W. Schwenke, H. Partridge, J. Chem. Phys. 113 (2000) 6592–6597.
[23] S. Mikhailenko, S. Tashkun, T. Putilova, E. Starikova, L. Daumont, A. Jenouvrier, S. Fally, M. Carleer, C. Hermans, A. Vandaele, J. Quant. Spectrosc. Radiat. Trans. 110 (2009) 597–608.
[24] A. Liu, O. Naumenko, S. Kassi, A. Campargue, J. Quant. Spectrosc. Radiat. Trans. 110 (2009) 1781–1800.
[25] S. Mikhailenko, S. Tashkun, L. Daumont, A. Jenouvrier, M. Carleer, S. Fally, A. Vandaele, J. Quant. Spectrosc. Radiat. Trans. 111 (2010) 2185–2196.
[26] P. Ormsby, K. Rao, M. Winnewisser, B. Winnewisser, O. Naumenko, A. Bykov, L. Sinitsa, J. Mol. Spectrosc. 158 (1993) 109–130.
[27] A.-W. Liu, K.-F. Song, H.-Y. Ni, S.-M. Hu, O.V. Naumenko, I.A. Vasilenko, S.N. Mikhailenko, J. Mol. Spectrosc. 265 (2011) 26–38.
[28] H.-Y. Ni, A.-W. Liu, K.-F. Song, S.-M. Hu, O. Naumenko, T. Kruglova, S. Tashkun, Mol. Phys. 106 (2008) 1793–1801.
[29] G. Mellau, S. Mikhailenko, E. Starikova, S. Tashkun, H. Over, V. Tyuterev, J. Mol. Spectrosc. 224 (2004) 32–60.
[30] S.V. Shirin, N.F. Zobov, O.L. Polyansky, J. Quant. Spectrosc. Radiat. Trans. 109 (2008) 549–558.
[31] A.A. Ruth, J. Orphal, S.E. Fiedler, Appl. Opt. 46 (2007) 3611–3616.
[32] S.E. Fiedler, A. Hese, A.A. Ruth, Chem. Phys. Lett. 371 (2003) 284–294.
[33] L.S. Rothman, I.E. Gordon, A. Barbe, D.C. Benner, P.F. Bernath, M. Birk, V. Boudon, L.R. Brown, A. Campargue, J.-P. Champion, K. Chance, L.H. Coudert, V. Dana, V.M. Devi, S. Fally, J.-M. Flaud, R.R. Gamache, A. Goldman, D. Jacquemart, I. Kleiner, N. Lacome, W.J. Lafferty, J.-Y. Mandin, S.T. Massie, S.N. Mikhailenko, C.E. Miller, N. Moazzen-Ahmadi, O.V. Naumenko, A.V. Nikitin, J. Orphal, V.I. Perevalov, A. Perrin, A. Predoi-Cross, C.P. Rinsland, M. Rotger, M. imekov, M.A.H. Smith, K. Sung, S.A. Tashkun, J. Tennyson, R.A. Toth, A.C. Vandaele, J.V. Auwera, J. Quant. Spectrosc. Radiat. Trans. 110 (2009) 533–572.
[34] J. Tennyson, M.A. Kostin, P. Barletta, G.J. Harris, O.L. Polyansky, J. Ramanlal, N.F. Zobov, Comput. Phys. Comm. 163 (2004) 85–116.
[35] I.I. Bubukina, N.F. Zobov, O.L. Polyansky, S.V. Shirin, S.N. Yurchenko, Opt. Spect. 110 (2011) 160–166.
[36] L. Lodi, J. Tennyson, O.L. Polyansky, J. Chem. Phys. 135 (2011) 034113.
[37] S.N. Yurchenko, B.A. Voronin, R.N. Tolchenov, N. Doss, O.V. Naumenko, W. Thiel, J. Tennyson, J. Chem. Phys. 128 (2008) 044312.
[38] L. Lodi, R.N. Tolchenov, J. Tennyson, A.E. Lynas-Gray, S.V. Shirin, N.F. Zobov, O.L. Polyansky, A.G. Császár, J. van Stralen, L. Visscher, J. Chem. Phys. 128 (2008) 044304.
[39] N.F. Zobov, S.V. Shirin, R.I. Ovsyannikov, O.L. Polyansky, S.N. Yurchenko, R.J. Barbe, J. Tennyson, R. Hargreaves, P. Bernath, J. Mol. Spectrosc. 269 (2011) 104–108.
[40] O.L. Polyansky, N.F. Zobov, S. Viti, J. Tennyson, P.F. Bernath, L. Wallace, Astrophys. J. 489 (1997) L205–L208.
[41] S. Mikhailenko, O. Naumenko, A. Nikitin, I. Vasilenko, A.-W. Liu, K.-F. Song, H.-Y. Ni, S.-M. Hu, J. Quant. Spectrosc. Radiat. Trans. 113 (2012) 653–669.
[42] A.-W. Liu, J.-H. Du, K.-F. Song, L. Wang, L. Wan, S.-M. Hu, J. Mol. Spectrosc. 237 (2006) 149–162.
[43] H.-Y. Ni, A.-W. Liu, K.-F. Song, S.-M. Hu, O. Naumenko, T. Kruglova, S. Tashkun, Mol. Phys. 106 (2008) 1793–1801.